

Perturbative triples correction for the equation-of-motion coupled-cluster wave functions with single and double substitutions for ionized states: Theory, implementation, and examples

Prashant U. Manohar,¹ John F. Stanton,² and Anna I. Krylov^{1,a)}¹*Department of Chemistry, University of Southern California, Los Angeles, California 90089-0482, USA*²*Department of Chemistry, University of Texas, Austin, Texas 78712, USA*

(Received 24 June 2009; accepted 27 August 2009; published online 18 September 2009)

A noniterative N^6 triples energy correction is presented for the equation-of-motion coupled-cluster method with single and double substitutions for ionized states (EOM-IP-CCSD). The correction, which is size intensive, is derived using a second-order Rayleigh–Schrödinger perturbative treatment and is similar to the approach of Stanton and Gauss [Theor. Chim. Acta **93**, 303 (1996)]. In the present implementation, only the target EOM-IP states are corrected, and the reference state is described by CCSD; the method is therefore more useful for the study of the target states themselves than ionization potentials. The performance of the correction, which demonstrates the caveat above, is demonstrated by applications to singlet methylene, BNB^- , nitrogen, carbon monoxide, acetylene, benzene, thymine, and adenine. © 2009 American Institute of Physics. [doi:10.1063/1.3231133]

I. INTRODUCTION

The equation-of-motion (EOM) coupled-cluster (CC)^{1–17} methods provide efficient and robust computational tools for many systems with strongly interacting electronic states. EOM-CC methods are similar, or equivalent, to several other approaches, such as linear response CC,^{18–22} symmetry-adapted cluster configuration interaction (CI),^{23,24} and certain classes of multireference (MR) CC methods.^{25–30} An advantage of EOM-CC is that it simultaneously treats both static and dynamic correlations of the target state and is based on a straightforward single-reference formalism. Moreover, it obtains energies and wave functions for all states of interest through diagonalization of a transformed Hamiltonian matrix, which endows it with properties that are usually associated only with “true” multireference approaches, specifically a balanced treatment of the most important electron configurations that contribute to a correlated wave function.

Typical errors in excitation energies associated with “single excitation processes” for EOM-EE-CC with single and double substitutions are in the 0.1–0.3 eV range,³¹ with a pronounced tendency for systematic overestimation. However, the energy gaps between the states are generally more accurate than the absolute positions relative to the ground state. Equivalently, the potential surfaces calculated for the various target states tend to be somewhat better than excitation energies. These methods are quite well suited to study properties of the target states, in addition to the most common applications in which just energy differences are calculated.^{32–35}

In addition to the calculation of excitation energies, the methods known as EOM-IP-CC and EOM-EA-CC are designed to calculate target states with one fewer (IP), or one

more (EA), electron than in the reference state. In the case of ionized (or electron-attached) states, the target ($N-1/N+1$)-electron configurations are decoupled from the N -electron reference and the resulting wave functions and energies are rigorously size intensive at any level of approximation, unlike the corresponding EE models.³⁶ Errors in EOM-IP and EOM-EA are quite comparable to those found in the corresponding EOM-EE calculations, which is expected since the methods are formally equivalent and have the property that a Rydberg series calculated with the EOM-EE approach with a sufficiently diffuse basis will converge to the corresponding root of the EOM-IP equations. However, due to the somewhat more ferocious nature of orbital relaxation when an electron is removed (as opposed to excited), errors in the EOM-IP and EOM-EA methods can be slightly greater than those characteristically found in EOM-EE calculations.³⁷ For satellite states (in which ionization is accompanied by excitation of one of the remaining electrons), the errors can be very large. This is similar to the case in EOM-EE, when doubly excited states are studied. Fortunately, in single-photon spectroscopy, the states best described by the EOM methods—the so-called Koopmans states (principal ionizations) and the excited states dominated by a single electron promotion—are also those that are most prominent (and important) in spectra. In EOM-IP, which is the subject of the present study, energy gaps between the low-lying ionized states are also more accurately predicted than the ionization energies, e.g., in a benchmark study of several small systems differences between EOM-IP-CCSD and full configuration interaction (FCI) for energy differences between the $N-1$ electron states were found to be less than 0.05 eV.¹⁷

The most straightforward way to improve accuracy is to include triple excitations in both the CC and EOM amplitudes. The resulting EOM-IP-CCSDT^{37–40} method describes

^{a)}Electronic mail: krylov@usc.edu.

the principal and satellite states with an accuracy of ~ 0.05 and ~ 0.5 eV, respectively. However, the N^8 scaling of CCSDT (for the reference state calculation) limits the applicability of EOM-IP-CCSDT to only small molecules and/or modest basis sets. This bottleneck motivated the development of approximate methods^{8,13,16,41–45} for including triple excitations in the EOM-CCSD ansatz. Following a similar EOM-EE method, Hirata *et al.*⁴³ introduced EOM-IP-CC(2,3), which was also implemented by Krylov and co-workers⁴⁵ and applied to study Jahn–Teller distortions and bonding in the benzene dimer cations. In this approach, the CC amplitudes are truncated at double substitutions, whereas the EOM amplitudes include up to triple substitutions, i.e., $3h2p$ (three holes two particles). The resulting N^7 scheme improves the energy differences between, and overall description of, the ionized states; IEs are of course systematically underestimated due to neglect of the additional reference state correlation. Because the method is iterative, the storage of five-index EOM amplitudes (although less demanding compared to the corresponding six-index quantities in the EE and related spin flip, or SF, methods) cannot be avoided, which limits the applications to relatively small systems.

One of the first noniterative corrections to EOM-IP-CCSD was introduced by Stanton and Gauss,⁸ which was based on a perturbation analysis. The CCSD energy of the reference state is perturbatively complete to the third order, whereas the EOM-IP states are not.⁸ The correction of Stanton and Gauss,⁸ as well as the more recent EOM-IP-CCSD* ansatz of Stanton and co-workers,⁴¹ improves the description of the ionized states reducing the error bars for energy differences between the ionized states to 0.01 eV. Similar developments in MRCC have been pursued by Pal *et al.*⁴⁶ and, more recently, by Sinha and co-workers.⁴⁷ However, the IEs are not improved because no similar correction is applied to the reference state. The virtues of the method are therefore in studying final state properties, rather than ionization energies.

Balanced inclusion of triple excitations in EOM-IP-CC is not straightforward, except for the full EOM-IP-CCSDT scheme. The overall effect of explicit triple excitations is to lower the IEs relative to EOM-IP-CCSD values.^{37–39} When both the reference and ionized states are treated as zeroth-order and are corrected using the same perturbative treatment (as described below), the reference-state energy is lowered more than the ionized state energies, which leads to overestimated IEs. Conversely, complete neglect of the correction to the reference state as in EOM-IP-CC(2,3) overcorrelates the target states relative to the reference, and the resulting IEs are too low. Thus, a perturbative approximation to EOM-IP-CC(2,3) is expected to produce IEs that are in between EOM-IP-CCSD and EOM-IP-CC(2,3) and therefore closer to the more rigorous EOM-IP-CCSDT values by virtue of error cancellation.

This work presents a noniterative N^6 triples correction for the EOM-IP-CCSD energies derived by second-order Rayleigh–Schrödinger (RS) perturbation treatment of the similarity-transformed CCSD Hamiltonian, following our earlier work on the perturbative correction to the EOM-SF-

CCSD wave functions.⁴⁸ Our formalism and the resulting correction are similar to the perturbation approach of Stanton and Gauss.⁸ The EOM-IP-CCSD* correction of Stanton and co-workers⁴¹ can be derived from the present correction by further approximations based on perturbative arguments. The correction is applied to the target $N-1$ electron states only; therefore, it improves energy gaps between the ionized states, while yielding only modest improvement of IEs. Thus, the main goal of this work is to investigate an approach that ultimately will be most useful in the improvement of final-state description.

The structure of the paper is as follows. Section II presents the theoretical approach. In Sec. III, we discuss the calculations of IEs of methylene, NB_2^- anion, nitrogen, carbon monoxide, acetylene, benzene, thymine, and adenine. The implementation and programmable expressions are presented in the Appendices A and B.

II. THEORY

We begin by considering the CCSD similarity-transformed Hamiltonian \bar{H} :

$$\bar{H} = e^{-(T_1+T_2)} H e^{T_1+T_2}, \quad (1)$$

where T_1 and T_2 operators generate all singly and doubly excited determinants from an N -electron closed-shell reference Φ_0 and satisfy the CC equations for the reference state. The $(N-1)$ states are obtained by an electron-removing operator acting on the reference state:

$$|\Phi^{(N-1)}\rangle = R^{IP} |\Phi_0^{(N)}\rangle, \quad (2)$$

$$\langle \Phi^{(N-1)} | = \langle \Phi_0^{(N)} | L^{IP},$$

where

$$\begin{aligned} R^{IP} &= R_1^k + R_2^k + \dots \\ &= \sum_i r_i i + \frac{1}{2} \sum_{ija} r_{ij}^a a^+ j i + \dots, \end{aligned} \quad (3)$$

$$\begin{aligned} L^{IP} &= L_1^k + L_2^k + \dots \\ &= \sum_i l_i i^+ + \frac{1}{2} \sum_{ija} l_{ij}^a i^+ j^+ a + \dots. \end{aligned} \quad (4)$$

The ionization energy of the k th target state can be given as the commutator equation:

$$[\bar{H}, R^k] |\Phi_0\rangle = (E_k - E_0) |\Phi_0\rangle. \quad (5)$$

Similar to the excited states, the ionized states are obtained by diagonalizing \bar{H} in the space of the target determinants, i.e., $(N-1)$ electron configurations. Diagonalization of the $\{S, D\}$ block of the ionized space (i.e., $1h$ and $2h1p$ determinants) yields the EOM-IP-CCSD ionization energies and wave functions:

$$\bar{H} R^k |\Phi_0\rangle = E_k R^k |\Phi_0\rangle, \quad (6)$$

$$\langle \Phi_0 | L^k \bar{H} = \langle \Phi_0 | L^k E_k. \quad (7)$$

Because \bar{H} is non-Hermitian, its left and right eigenstates are not complex conjugates of each other but can be chosen to form a biorthogonal set:

$$\langle \Phi_0 | L^k | R^l \Phi_0 \rangle = \delta_{kl}. \quad (8)$$

By splitting \bar{H} into a zero-order part H_0 (to be specified later) and the perturbation $V \equiv \bar{H} - H_0$ and generalizing second-order RS perturbation theory to a non-Hermitian Hamiltonian, we arrive to the following general expressions:⁴⁸

$$H_0 |\Psi_k^{(0)}\rangle = E_k^{(0)} |\Psi_k^{(0)}\rangle, \quad (9)$$

$$\langle \tilde{\Psi}_k^{(0)} | H_0 = E_k^{(0)} \langle \tilde{\Psi}_k^{(0)} |, \quad (10)$$

$$E_k^{(1)} = \langle \tilde{\Psi}_k^{(0)} | V | \Psi_k^{(0)} \rangle, \quad (11)$$

$$(H_0 - E_k^{(0)}) |\Psi_k^{(1)}\rangle = -(V - E_k^{(0)}) |\Psi_k^{(0)}\rangle, \quad (12)$$

$$E_k^{(2)} = \langle \tilde{\Psi}_k^{(0)} | V | \Psi_k^{(1)} \rangle, \quad (13)$$

where left $\langle \tilde{\Psi}_k^{(0)} |$ and right $|\Psi_l\rangle$ eigenfunctions satisfy the following conditions:

$$\langle \tilde{\Psi}_k^{(0)} | \Psi_l^{(0)} \rangle = \delta_{kl}, \quad (14)$$

$$\langle \tilde{\Psi}_k^{(0)} | \Psi_k^{(1)} \rangle = 0. \quad (15)$$

We define H_0 such that $E_k^{(0)}$ and $\Psi_k^{(0)}$ correspond to the EOM-IP-CCSD energies and wave functions, as in the works of Stanton and Gauss,⁸ Hirata *et al.*,¹³ and our derivation of the EOM-SF correction.⁴⁸ Since the reference state is decoupled from the ionized states, the ionized block of Hamiltonian can be diagonalized separately. Thus, the matrix of H_0 is block diagonal: in the $\{S, D\}$ block, it is simply the matrix of \bar{H} in the basis of the $1h$ and $2h1p$ determinants. In this work, the zeroth-order part of \bar{H} in the external space (triply and more highly excited determinants) is defined to include only terms along the diagonal.

Various choices for the external and diagonal part of H_0 can be made, of which two are studied here. First, the “(dT)” correction, in which all \bar{H} terms are included along the diagonal, and second, the “(fT)” correction, in which just the bare Fock matrix contribution is included (the usual Møller–Plesset form). Considering for the moment only the triply excited determinants, the two choices are,

$$\langle T | H_0 | T \rangle = \langle \Phi_{ijk}^{ab} | \bar{H} | \Phi_{ijk}^{ab} \rangle, \quad (16)$$

$$\langle T | H_0 | T \rangle = \langle \Phi_{ijk}^{ab} | F | \Phi_{ijk}^{ab} \rangle. \quad (17)$$

The computational costs of (dT) and (fT) are very similar and in fact are identical, apart from a noniterative step in which the somewhat less trivial (dT) denominators are formed.

The off-diagonal blocks of V are the projections of \bar{H} onto the external space

$$\langle T | V | \Phi_0 \rangle = \langle \Phi_{ijk}^{ab} | \bar{H} | \Phi_0 \rangle, \quad (18)$$

$$\langle Q | V | \Phi_0 \rangle = \langle \Phi_{ijkl}^{abc} | \bar{H} | \Phi_0 \rangle. \quad (19)$$

By virtue of the block-diagonal form of H_0 , the first-order energy correction is zero and the first order correction to the wave functions, $\Psi_k^{(1)}$, does not include the reference, singly ($1h$) or doubly ($2h1p$) excited determinants.⁴⁹ The amplitudes of triple and quadruple excitations are defined by Eq. (12).

At this point, we restrict the external space to just triple excitations. While in the perturbative arguments of the Stanton–Gauss approach, a restriction to triples is a rigorous consequence of the theory, using the entire \bar{H} as $H_0 + V$ leads to the consequence that quadruples contribute at second order. This has been done in the so-called CCSD(2) method in a factorized form,^{50,51} but there is ample evidence^{52–56} that triples-only perturbative corrections work sufficiently well that quadruples can be neglected with no significant penalty in accuracy.

After restricting attention to triple excitations, we arrive at

$$\Psi_m^{(1)} = \frac{1}{(3!2!)} \sum_{ijkab} R_{ijk}^{ab} \Phi_{ijk}^{ab}, \quad (20)$$

$$R_{ijk}^{ab} = -\frac{\sigma_{ijk}^{ab}}{D_{ijkab}^m}, \quad (21)$$

$$\sigma_{ijk}^{ab} = [\langle \Phi_{ijk}^{ab} | \bar{H} | R_1 \Phi_0 \rangle + \langle \Phi_{ijk}^{ab} | \bar{H} | R_2 \Phi_0 \rangle], \quad (22)$$

$$D_{ijkab}^m = \langle \Phi_{ijk}^{ab} | \bar{H} | \Phi_{ijk}^{ab} \rangle - E_m^{(0)}. \quad (23)$$

Note that σ_{ijk}^{ab} are the same as the right σ vectors for the Davidson procedure in EOM(2,3) minus the contributions from the triply excited EOM(2,3) amplitudes. By combining the above with Eq. (13), the second-order energy correction assumes the following form:

$$E_m^{(2)} = -\frac{1}{(3!2!)} \sum_{ijkab} \frac{\tilde{\sigma}_{ijk}^{ab} \sigma_{ijk}^{ab}}{D_{ijkab}^m} \\ = -\frac{1}{(3!2!)} \sum_{ijkab} \frac{\langle \Phi_0 | L^m | \bar{H} | \Phi_{ijk}^{ab} \rangle \langle \Phi_{ijk}^{ab} | \bar{H} | R^m \Phi_0 \rangle}{D_{ijkab}^m}, \quad (24)$$

where L^k and R^k are the left and right EOM-CCSD eigenvectors for state $k \neq 0$, respectively.

The $\tilde{\sigma}$ and σ vectors in the above equation are given by:

$$\tilde{\sigma}_{ijk}^{ab} = \langle \Phi_0 | L_1 | \bar{H} | \Phi_{ijk}^{ab} \rangle + \langle \Phi_0 | L_2 | \bar{H} | \Phi_{ijk}^{ab} \rangle, \quad (25)$$

$$\sigma_{ijk}^{ab} = \langle \Phi_{ijk}^{ab} | \bar{H} | R_1 \Phi_0 \rangle + \langle \Phi_{ijk}^{ab} | \bar{H} | R_2 \Phi_0 \rangle. \quad (26)$$

Using the intermediates given in Appendix B, the right hand side quantities in Eqs. (25) and (26) can be expanded to obtain the programmable expressions for $\tilde{\sigma}$ and σ :

$$\langle \Phi_0 | L_1 | \bar{H} | \Phi_{ijk}^{ab} \rangle = P(i|jk)P(a|bc)t_{ijk}^a \langle jk | bc \rangle, \quad (27)$$

$$\begin{aligned} \langle \Phi_0 L_2 | \bar{H} | \Phi_{ijk}^{ab} \rangle &= P(i|jk)P(ab)t_{jk}^b F_{ia} \\ &\quad - P(i|jk)P(ab) \sum_l t_{il}^a t_{jklb}^6 \\ &\quad + P(ij|k) \sum_d t_{ij}^d t_{kdab}^7, \end{aligned} \quad (28)$$

$$\langle \Phi_{ijk}^{ab} | \bar{H} | R_1 \Phi_0 \rangle = P(ij|k) \left(\sum_l t_{kl}^{ab} H_{ijl}^2 + \sum_d t_{ij}^{ad} H_{kdb}^3 \right), \quad (29)$$

$$\begin{aligned} \langle \Phi_{ijk}^{ab} | \bar{H} | R_2 \Phi_0 \rangle &= P(ij|k) \left[\sum_d (r_{ij}^d t_{kdba}^3 + P(ab)t_{ij}^{ad} H_{kdb}^5) \right. \\ &\quad \left. + \sum_l (P(ab)r_{kl}^a t_{ijlb}^2 + t_{kl}^{ab} H_{ijl}^4) \right]. \end{aligned} \quad (30)$$

The diagonal D_{ijkab}^m from Eq. (24) is

$$\begin{aligned} D_{ijkab}^m &= \langle \Phi_{ijk}^{ab} | \bar{H} | \Phi_{ijk}^{ab} \rangle - (E_{CC} + \omega_m) \\ &= -P(ijk)F_{ii} + P(ab)F_{aa} + 2P(ij|k)I_{ijij}^4 \\ &\quad + 2P(ab|c)I_{abab}^5 - P(i|jk)P(a|bc)I_{iaia}^1 - P(ij|k) \\ &\quad \times \left[P(ab) \sum_d t_{ij}^{ad} \langle ij || ad \rangle + \sum_l t_{kl}^{ab} \langle kl || ab \rangle \right] - \omega_m, \end{aligned} \quad (31)$$

where E_{CC} and ω_m are the total reference-state CCSD and the EOM-IP-CCSD ionization energies, respectively. Note that the diagonal is symmetric with respect to permutation of indices, whereas the left and the right sigmas are antisymmetric.

None of the noniterative triples corrections is invariant with respect to the rotations within virtual or occupied subspaces. An important practical question is whether or not there is an unambiguous orbital choice upon which the resulting correction is invariant. Using bare orbital energy denominators and canonical orbitals, Eq. (16) is one of such safe and well-defined choices, whereas using the full diagonal, Eq. (17) is not invariant in the case of degenerate virtual orbitals. A simple solution to this problem, diagonalizing \bar{H} blocks in the subspace of degenerate orbitals, has been suggested by Piecuch and Włoch.⁵⁷

As follows from our choice of $H_0 + V$, the (fT) and (dT) methods can also be described as a perturbative approximation to the EOMIP-CC(2,3) method.⁵⁸ Both EOMIP-CCSD(dT) and EOMIP-CCSD(fT) energies and energy differences are size intensive.

The (fT) method is the same as that of EOMIP-CCSD*, except that instead of using the full \bar{H} matrix as V , Stanton and co-workers included only terms that contributed to the third-order energy, using a perturbation formalism that treats R_1 and L_1 as zeroth-order, T_1 as first-order, and T_2 as second-order. Their method, via the choice of order definition, is clearly designed only for principal ionization states. Our approach does not attempt to perturbatively deconstruct the \bar{H} matrix.

Note that Eq. (24) can be applied to the reference CCSD state, as discussed in detail in Ref. 48. The resulting corrections are identical to the CR-CCSD(T)_L method of Piecuch

*et al.*⁵⁶ derived using method-of-moments approach, or its CR-CCSD(T)₂ approximation. The latter has been also derived by Hirata *et al.*¹³ These corrections are size consistent and more robust as compared to (T). The corresponding derivation based on the Stanton–Gauss ansatz leads instead to what has been called aCCSD(T) (Ref. 54) and CCSD(T)_Δ,⁵⁵ which are equivalent and intermediate in quality between CCSD(T) and CR-CCSD(T)_L. aCCSD(T) can also, after another perturbative approximation, be shown to be equivalent to the ubiquitous CCSD(T) method.^{52,53} Similar corrections exploiting left eigenvalues of \bar{H} and including a factorized quadruple excitations has been developed by Gwaltney and co-workers.^{50,51}

III. RESULTS AND DISCUSSION

In order to reduce the amount of column space devoted to acronyms, we will adhere to the following shorthand notation for the rest of the presentation: the full EOM-IP-CCSD, EOM-IP-CCSDT, etc., methods will be abbreviated by SD, SDT, etc., while the EOM-IP-CCSD*, EOM-IP-CC(2,3), EOM-IP-CCSD(fT), EOM-IP-CCSD(dT) methods will be denoted as SD*, (2,3), (fT), and (dT), respectively; (xT) will be used as a generic to designate either of the methods developed in this work.

The latter methods have been tested for several molecular systems, ranging from standard small-molecule examples such as N₂ and CO, to acetylene, and more challenging systems such as benzene, adenine, and thymine. For the systems above, the ionization energies are of interest and such results are analyzed. To illustrate a case where the emphasis is exclusively on the final state, we document calculations on the anion of the BNB molecule; the associated (neutral) final states are part of a highly coupled vibronic system that attracted some interest in the theoretical community. For benzene and the two nucleic acids, we carry out calculations for both the vertical and more experimentally relevant adiabatic IEs.

A. Computational details

Calculations for methylene (\tilde{a}^1A_1) and the BNB anion were performed with the cc-pVDZ (Ref. 59) basis set with core orbitals frozen at the respective CCSD(T) equilibrium geometries (see EPAPS supplement⁶⁰).

Calculations for nitrogen, carbon monoxide and acetylene used a hierarchy of Dunning's correlation-consistent basis sets, i.e., cc-pVDZ, cc-pVTZ, and cc-pVQZ,⁵⁹ with geometries from Refs. 37 and 39: $R = 1.097\ 685$ and $1.128\ 323$ Å for nitrogen and carbon monoxide, respectively; and $R_{CC} = 1.203$ Å and $R_{CH} = 1.061$ Å for acetylene. The results for N₂, CO, and C₂H₂ have been extrapolated to obtain the IEs at the complete basis-set (CBS) limit^{61–66} using the formula⁶² employed by Kamyia and Hirata³⁷ in their benchmark study:

$$E(n) = E(\infty) + \eta_1 e^{-(n-1)} + \eta_2 e^{-(n-1)^2}, \quad (32)$$

where $E(\infty)$ is the energy at the CBS limit, and $n=2, 3, 4$ corresponds to the cc-pVDZ, cc-pVTZ, and cc-pVQZ basis sets, respectively. $E(n)$ are the corresponding energies, and η_1 and η_2 are parameters that are fit to the energies. Except

TABLE I. Vertical ionization energies (eV) of methylene (\bar{a}^1A_1), cc-pVDZ.

	1^2A_1	2^2B_2	2^2A_1
CCSD	10.271	14.693	22.381
CCSD(<i>f</i> T)	10.248	14.642	22.202
CCSD(<i>d</i> T)	10.232	14.620	22.143
CCSD*	10.238	14.628	22.157
CCSDT	10.294	14.623	21.963
CCSDTQ	10.298	14.617	21.919
CCSDTQP	10.298	14.617	21.918
FCI	10.298	14.617	21.918

for the satellite states of nitrogen and carbon monoxide, the core orbitals were frozen in the correlated calculations.

In the benzene calculations, we employ the cc-pVTZ (Ref. 59) basis set with the frozen-core approximation. The equilibrium geometry of benzene ($r_{CC}=1.3915$ Å and $r_{CH}=1.0800$ Å) is from Ref. 67, whereas the EOM-IP-CCSD/6-311G* optimized geometries for the 2^2B_{2g} and 2^2B_{3g} used to calculate the respective adiabatic ionization potentials are from Pieniazek *et al.*³⁴

For thymine and adenine, the geometries of the neutral molecules are optimized using RI-MP2 and cc-pVTZ (Ref. 59) basis set, whereas the cation geometries are optimized using IP-CISD method⁶⁸ with the 6-31+G(*d*) basis set.⁶⁹ For thymine, we present two sets of IEs computed with the original cc-pVTZ basis set,⁵⁹ and using a reduced basis set obtained from cc-pVTZ by removing *f*-functions for the second row elements and *d*-function for the hydrogen. The IEs of adenine are computed using the reduced cc-pVTZ basis set only. For both molecules, the core orbitals were frozen in the correlated calculations.

Molecular structures, relevant energies, and molecular orbitals are given in the EPAPS supplement.⁶⁰ The calculations are performed using the Q-CHEM electronic structure package⁷⁰ and CFOUR^{71,72} program.

B. Methylene

Table I summarizes the vertical IEs of singlet methylene. Except for the lowest IE, which corresponds to the 1^2A_1 cation state, the (*x*T) and SD* IEs are closer to full CI than the corresponding SD results. The absolute errors for SD IEs range from 0.027 to 0.46 eV. The (*f*T) and (*d*T) absolute errors are 0.025–0.28 and 0.003–0.23 eV, respectively; and the absolute error for SD* ranges from 0.011 to 0.24 eV. Absolute errors for SDT are 0.006–0.045 eV, whereas the SDTQ and SDTQP IEs are within 0.001 eV of the respective FCI values.

(*x*T) and SD* reduce the SD errors in the energy gaps between the states by 25%–35%, whereas SDT reduces the errors almost by an order of magnitude. The general trend for the errors is $SD > (fT) > SD^* > (dT) > SDT$.

C. BNB

The BNB molecule presents a notorious case of vibronic coupling between the $2^2\Sigma_u$ ground state and the low-lying $2^2\Sigma_g$ excited state,⁷³ which lies less than 1 eV above. This coupling and its manifestation in what is often called “artificial

TABLE II. Total energy (hartree) of the lowest ($2^2\Sigma_u$) state and the relative energy (eV) of $2^2\Sigma_g$ state of NB₂ at the equilibrium geometry of the anion, cc-pVDZ.

	$2^2\Sigma_u$	$2^2\Sigma_g$
CCSD	−103.997 60	0.734
CCSD(<i>f</i> T)	−104.004 65	0.719
CCSD(<i>d</i> T)	−104.006 28	0.718
CCSD*	−104.006 15	0.714
CCSDT	−104.020 89	0.699
CCSDTQ	−104.022 09	0.694

symmetry breaking” has confounded all but the most sophisticated⁷⁴ attempts at straightforward single reference calculations.⁷³ This problem, however, is readily accessible through EOM-IP-CC methods and presents a potentially ideal application of the approaches advanced in this paper. While further discussion of the coupling issues and comparison with experiment are well beyond the scope of this work, it suffices to say here that it is important for methods to predict the vertical gap between the two states well. Table II illustrates the performance of the various methods where we see that for the $\Sigma_u \rightarrow \Sigma_g$ gap, the SD, (*f*T), (*d*T), and SD* errors are 0.040, 0.025, 0.024, and 0.02 eV, respectively, whereas the SDT error with respect to the CCSDTQ value is negligibly small (i.e., 0.005 eV).

D. Nitrogen, carbon monoxide, and acetylene

The IEs of the isoelectronic molecules nitrogen, carbon monoxide, and acetylene are summarized in Tables III–V, respectively. The trend for Koopmans states of these molecules in all three basis sets is the same:

$$E_{SD} > E_{(fT)} > E_{(dT)} \sim E_{(2,3)} < E_{SDT}, \quad (33)$$

and, thus, it also holds at the extrapolated CBS limit. The (*x*T) correction reduces the EOM-IP-CCSD IE values by 0.1–0.35 eV.

Figures 1–3 show the deviations of the SD, (*f*T), (*d*T), and SD* values for IEs from the reference SDT values. As expected, (2,3), (*x*T) and SD* underestimate IEs because they do not include triples in the reference state. We considered using Eq. (24) to correct the ground state energy; however, this approach does not improve IEs because it overcorrelates the reference relative to the EOM states (typical values of the (*x*T) correction for the reference state are ~ 0.6 eV). The SD values for principal IEs are higher than the SDT values by 0.1–0.3 eV for all these molecules, whereas the (2,3) underestimates the IEs by about 0.3 eV. The (*f*T) correction underestimates the IEs corresponding to the Koopmans $2^2\Pi$ states in all the molecules by 0.13–0.22 eV with respect to the SDT values, whereas (*d*T) underestimates the IEs by additional 0.01–0.05 eV.

The effect of triple excitations is more prominent for the satellite $2^2\Pi$ state of CO, for which the SD error is 2–3 eV, whereas the corresponding (*f*T) and (*d*T) absolute errors (with respect to SDT) are 0.6 and 0.9 eV, respectively. These larger errors are expected due to the doubly excited ($2h1p$) character of the satellite states.^{75,76}

TABLE III. Vertical ionization energies (eV) of nitrogen.

Basis	Method	$\tilde{X}^2\Sigma_g^+$	$\tilde{A}^2\Pi_u$	$\tilde{B}^2\Sigma_u^+$	$\tilde{C}^2\Sigma_u^+$
cc-pVDZ	EOM-IP-CCSD	15.18	16.93	18.47	28.8
	EOM-IP-CCSD(<i>f</i> T)	15.06	16.51	18.39	25.6
	EOM-IP-CCSD(<i>d</i> T)	15.03	16.40	18.38	24.4
	EOM-IP-CCSD*	15.01	16.45	18.36	25.1
	EOM-IP-CC(2,3)	14.96	16.46	18.21	25.1
	EOM-IP-CCSDT ^a	15.10	16.64	18.36	25.28
	EOM-IP-CCSDTQ ^a	15.06	16.63	18.28	24.99
cc-pVTZ	EOM-IP-CCSD	15.56	17.18	18.83	29.6
	EOM-IP-CCSD(<i>f</i> T)	15.37	16.71	18.67	25.8
	EOM-IP-CCSD(<i>d</i> T)	15.34	16.63	18.65	24.9
	EOM-IP-CCSD*	15.32	16.65	18.62	25.3
	EOM-IP-CC(2,3)	15.26	16.65	18.47	25.3
	EOM-IP-CCSDT ^a	15.44	16.90	18.67	25.63
	EOM-IP-CCSD	15.68	17.28	18.94	29.8
cc-pVQZ	EOM-IP-CCSD	15.46	16.79	18.76	25.8
	EOM-IP-CCSD(<i>f</i> T)	15.44	16.73	18.74	25.2
	EOM-IP-CCSD*	15.41	16.73	18.71	25.3
	EOM-IP-CC(2,3)	15.35	16.73	18.56	25.4
	EOM-IP-CCSDT ^a	15.55	16.99	18.77	25.76
	EOM-IP-CCSD	15.75	17.34	19.01	30.0
	EOM-IP-CCSD(<i>f</i> T)	15.51	16.83	18.81	25.9
CBS ^b	EOM-IP-CCSD	15.49	16.79	18.79	25.4
	EOM-IP-CCSD*	15.47	16.78	18.76	25.3
	EOM-IP-CC(2,3)	15.40	16.78	18.61	25.5
	EOM-IP-CCSDT ^a	15.61	17.05	18.83	25.83
	Experiment He(I) ^c	15.60	16.98	18.78	
	Experiment He(II) ^d	15.58	16.93	18.75	25.51
	Experiment XPS ^e	15.58	17.0	18.8	

^aFrom Ref. 37.^bCalculated using Eq. (32), see text.^cFrom Ref. 86.^dFrom Ref. 87.^eFrom Ref. 88.

For the $^2\Sigma$ states, (*x*T) gives more accurate results. The (*f*T) and (*d*T) IEs for the ground ($\tilde{X}\Sigma_g^+$) state of the nitrogen cation are underestimated by 0.1–0.12 eV with respect to the SDT values, whereas the IEs for $\tilde{B}\Sigma_u^+$ are within 0.02–0.2 eV from SDT. The (*f*T) and (*d*T) errors for the satellite state of nitrogen are different: the (*f*T) value is greater than the SDT one by 0.1 eV, whereas (*d*T) is 0.4 eV below.

Carbon monoxide exhibits similar behavior for the two $^2\Sigma^+$ states. The (*f*T) and (*d*T) errors for the ground ($\tilde{X}\Sigma^+$) state are –0.12 and –0.13 eV, respectively, whereas for the $\tilde{B}\Sigma^+$ state the errors are 0.04 and –0.03 eV, respectively. The (*f*T) and (*d*T) errors for the $\tilde{A}^2\Sigma_g^+$ state of acetylene are –0.08 and –0.09 eV, and for the $\tilde{B}^2\Sigma_g^+$ state, –0.02 and –0.03 eV, respectively.

In summary for CO and N₂ the errors with respect to EOM-IP-CCSDT for Koopmans states range between 0.04 and –0.2 eV for (*f*T) and between –0.03 and –0.3 eV for (*d*T). The EOM-IP-CCSD* errors are comparable to those of (*f*T) and (*d*T), however, they do not exhibit systematic trends with respect to (2,3) and SDT. The SD and (2,3) errors with respect to SDT range between 0.3 and –0.3 eV.

For the satellite states, the (*x*T) absolute error ranges

from 0.1 to 0.9 eV, which is 4–40 times less than CCSD error (3–4 eV). The SD* errors for the satellite states are comparable to the (2,3) errors. For nitrogen, the SD* and (2,3) absolute errors are 1.0 and 1.1 eV, respectively, whereas for CO the SD* error is greater than the (2,3) error (0.3 eV) by 0.2 eV. For these systems, the overall performance of (*f*T) is found to be more balanced (in a sense of error cancellation) than that of (*d*T) and SD* methods. The (*f*T) IEs are consistently in between the SD and (2,3) values and are, therefore, more accurate. The (*f*T) correction provides an accuracy of 0.1–0.2 eV for Koopmans' states whereas, for the satellite states, the error bar is ~1 eV.

The maximum absolute error for the energy differences between the principal ionized states for SD is ± 0.15 eV, and the (*x*T) and SD* values are similar. The (2,3) energy differences are very close to the SDT values.

E. Benzene

Total ground state energies and low-lying vertical and adiabatic IEs of benzene are given in Table VI. The corresponding molecular orbitals are given in the supplementary materials.⁶⁰ In the neutral, the σ^* and π^* orbitals feature

TABLE IV. Vertical ionization energies (eV) of carbon monoxide.

Basis	Method	$\tilde{X}^2\Sigma^+$	$\tilde{A}^2\Pi$	$\tilde{B}^2\Sigma^+$	$\tilde{D}^2\Pi$
cc-pVDZ	EOM-IP-CCSD	13.81	16.74	19.47	26.4
	EOM-IP-CCSD(<i>f</i> T)	13.51	16.66	19.43	23.6
	EOM-IP-CCSD(<i>d</i> T)	13.44	16.62	19.36	22.6
	EOM-IP-CCSD*	13.43	16.66	19.42	23.3
	EOM-IP-CC(2,3)	13.42	16.56	19.24	23.0
	EOM-IP-CCSDT ^a	13.58	16.71	19.33	24.00
	EOM-IP-CCSDTQ ^a	13.57	16.70	19.36	23.74
cc-pVTZ	EOM-IP-CCSD	14.13	17.02	19.74	26.9
	EOM-IP-CCSD(<i>f</i> T)	13.80	16.85	19.60	23.7
	EOM-IP-CCSD(<i>d</i> T)	13.75	16.80	19.53	23.0
	EOM-IP-CCSD*	13.71	16.84	19.59	23.4
	EOM-IP-CC(2,3)	13.70	16.74	19.39	23.2
	EOM-IP-CCSDT ^a	13.89	16.96	19.55	24.27
	EOM-IP-CCSD	14.22	17.13	19.86	27.1
cc-pVQZ	EOM-IP-CCSD(<i>f</i> T)	13.87	16.92	19.68	23.8
	EOM-IP-CCSD(<i>d</i> T)	13.85	16.88	19.62	23.3
	EOM-IP-CCSD*	13.79	16.92	19.67	23.4
	EOM-IP-CC(2,3)	13.78	16.81	19.46	23.3
	EOM-IP-CCSDT ^a	13.98	17.05	19.64	24.36
	EOM-IP-CCSD	14.27	17.19	19.92	27.2
	EOM-IP-CCSD(<i>f</i> T)	13.91	16.97	19.74	23.8
CBS ^b	EOM-IP-CCSD(<i>d</i> T)	13.90	16.92	19.67	23.5
	EOM-IP-CCSD*	13.83	16.96	19.72	23.4
	EOM-IP-CC(2,3)	13.83	16.85	19.51	23.3
	EOM-IP-CCSDT ^a	14.03	17.10	19.70	24.42
	Experiment He(I) ^c	14.01	16.91	19.72	
	Experiment He(II) ^d	14.01	16.91	19.69	23.4
	Experiment XPS ^e	14.01	17.0	19.7	23.6
Experiment EMS ^f	14.01	17.03	19.6	24.1	

^aFrom Ref. 37.^bCalculated using Eq. (32), see text.^cFrom Ref. 86.^dFrom Ref. 89.^eFrom Ref. 88.^fFrom Ref. 90.

twofold degeneracy, which is broken upon ionization. The E_{1g} , E_{2g} , and A_{2u} labels refer to the ionized states at the ground state geometry (D_{6h} symmetry), whereas B_{2g} and B_{3g} are the lowest adiabatic ionized states corresponding to the ionization in the π^* orbitals, whose degeneracy is broken due to the geometric distortion in the cation leading to the D_{2h} symmetry.

For vertical IEs, we also present experimental results.⁷⁷ The IEs are calculated in two ways: (i) using EOM-IP with the RHF reference of the neutral and (ii) as differences between the total CC energies of the cation and the neutral (referred to as ΔE). The former approach is size intensive, spin pure, and efficiently incorporates the multireference character of the ionized states, however, the latter is rigorously size extensive and includes higher-order terms from the perturbation theory point of view. For EOM methods, the (*f*T) and (*d*T) values lie systematically between the SD and (2,3) values.

As in the above examples, the IEs corresponding to the ionizations from the π bonding and antibonding orbitals are underestimated more by EOM-IP-CCSD(*x*T) than those for other states. For the E_{1g} state, the difference between the ΔE

and EOM values increases from -0.1 (SD) to 0.3 eV (*x*T). Whereas (*x*T) increases IE calculated as ΔE by ~ 0.05 eV, the respective EOM value decreases by about 0.25 eV. For the A_{2u} state, both EOM and ΔE yield lower IE upon inclusion of the perturbative correction, and the ΔE -EOM difference slightly increases from 0.22 to 0.29 eV for the (*f*T) correction, and decreases to 0.26 eV for (*d*T). For the E_{2g} state, (*f*T) and (*d*T) reduce the ΔE -EOM difference by 0.015 and 0.03 eV, respectively.

For the vertically ionized states, the only dipole-allowed transition is the $\pi \rightarrow \pi^*$ transition between the ${}^2E_{1g}$ and ${}^2A_{2u}$ states. The reported value⁷⁷ (estimated from vertical IEs) for this energy gap is 2.85 eV, which is considerably below all theoretical predictions. At the EOM-CCSD level, it is 3.35 eV, whereas with the (*x*T) correction it decreases by 0.1 eV. The EOM-CC(2,3) value is 3.010 eV. At all the CC levels, the ΔE calculation slightly overestimates the $\pi \rightarrow \pi^*$ EE relative to EOM-IP. The EOM versus ΔE difference for this energy at the CCSD level is 0.262 eV. The (*f*T) correction decreases the difference by one order of magnitude making it 0.026 eV, whereas the corresponding (*d*T) value is 0.028 eV.

TABLE V. Vertical ionization energies (eV) of acetylene.

Basis	Method	$\tilde{X}^2\Pi_u$	$\tilde{A}^2\Sigma_g^+$	$\tilde{B}^2\Sigma_u^+$
cc-pVDZ	EOM-IP-CCSD	11.33	16.99	18.90
	EOM-IP-CCSD(<i>f</i> T)	11.10	16.88	18.81
	EOM-IP-CCSD(<i>d</i> T)	11.10	16.86	18.81
	EOM-IP-CCSD*	11.08	16.84	18.77
	EOM-IP-CC(2,3)	11.06	16.79	18.68
	EOM-IP-CCSDT ^a	11.23	16.91	18.80
cc-pVTZ	EOM-IP-CCSD	11.54	17.21	19.12
	EOM-IP-CCSD(<i>f</i> T)	11.24	17.03	18.97
	EOM-IP-CCSD(<i>d</i> T)	11.21	17.02	18.97
	EOM-IP-CCSD*	11.21	16.99	18.92
	EOM-IP-CC(2,3)	11.19	16.93	18.83
	EOM-IP-CCSDT ^a	11.42	17.09	18.98
cc-pVQZ	EOM-IP-CCSD	11.61	17.29	19.19
	EOM-IP-CCSD(<i>f</i> T)	11.29	17.09	19.02
	EOM-IP-CCSD(<i>d</i> T)	11.27	17.08	19.02
	EOM-IP-CCSD*	11.26	17.05	18.97
	EOM-IP-CC(2,3)	11.24	16.99	18.88
	EOM-IP-CCSDT ^a	11.48	17.16	19.04
CBS ^b	EOM-IP-CCSD	11.66	17.34	19.23
	EOM-IP-CCSD(<i>f</i> T)	11.32	17.13	19.06
	EOM-IP-CCSD(<i>d</i> T)	11.31	17.12	19.05
	EOM-IP-CCSD*	11.29	17.08	19.01
	EOM-IP-CC(2,3)	11.26	17.02	18.91
	EOM-IP-CCSDT ^a	11.52	17.21	19.08
Experiment ^c		11.49	16.7	18.7

^aSee Ref. 39.^bCalculated using Eq. (32), see text.^cFrom Ref. 91.

In the case of the adiabatic IEs, the EOM and ΔE calculations behave differently. Whereas (*x*T) in the former decreases the IEs by 0.2–0.3 eV, in the latter it increases them by about 0.05 eV. The difference between the (*d*T) and (*f*T) values is very small in the ΔE calculations, since the wave functions for the neutral and ionized states are perturbatively compatible. The B_{2g} and B_{3g} states correspond to the ionizations from the two degenerate e_{1g} orbitals. For both relaxed geometries, the b_{2g} orbital lies slightly lower in energy than the b_{3g} orbital. The trend of energy difference between these states is similar to that of the vertically ionized states.

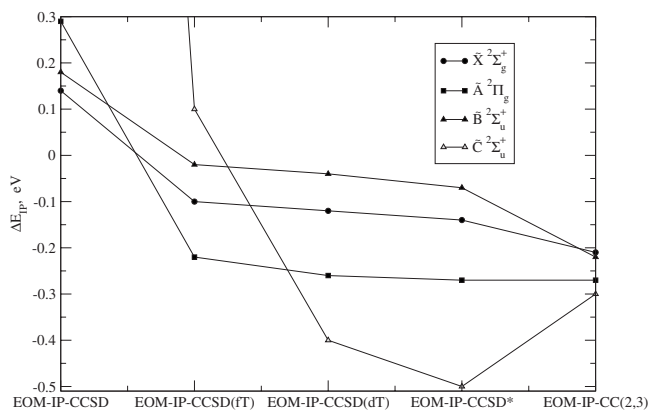


FIG. 1. Energy differences against EOM-IP-CCSDT ionization energies for nitrogen in the CBS limit.

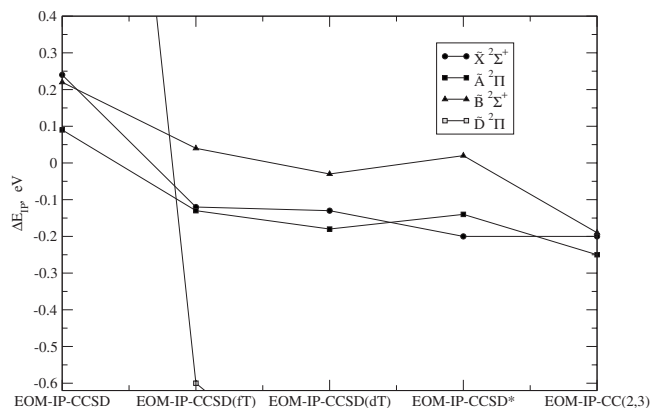


FIG. 2. Energy differences against EOM-IP-CCSDT ionization energies for carbon monoxide in the CBS limit.

F. Thymine

Vertical and adiabatic IEs of thymine computed with the cc-pVTZ and reduced cc-pVTZ basis sets are summarized in Table VII. The relevant MOs are given in the supplementary materials.⁶⁰ The (*x*T) values are systematically below (by ~ 0.3 eV) the corresponding SD values for both bases. The experimental values^{78–81} show the uncertainty of 0.05–0.2 eV. Whereas the vertical IEs at the CCSD level are systematically higher than the experimental values,^{78,79} the (*x*T) corrections underestimate the IEs except for the $3^2A''$ state. For this state, the SD error calculated with the cc-pVTZ basis set is 0.56 eV, whereas (*f*T) and (*d*T) reduce it to 0.184 and 0.077 eV, respectively. The errors for the energy spacing between the ionized states for SD, (*f*T), and (*d*T) are 0.458, 0.419, and 0.334 eV, respectively (for cc-pVTZ).

The removal of *f*-functions from the second row elements and *d*-functions from hydrogen decreases the IE values by about 0.1–0.12 eV at the SD level, whereas the (*x*T) values decrease by 0.08–0.11 eV. However, this does not affect the energy gaps between the ionized states, for which the errors are 0.467, 0.415, and 0.419 eV for the SD, (*f*T), and (*d*T) methods, respectively.

For the reduced cc-pVTZ basis set, we also present the IEs computed with (2,3). As in the case of nitrogen, carbon monoxide, and acetylene, the (*x*T) IEs are in between the SD and the (2,3) values. The (*x*T) IEs are higher than the corre-

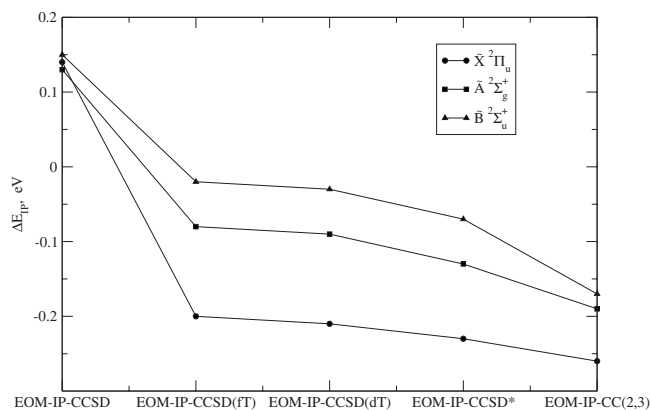


FIG. 3. Energy differences against EOM-IP-CCSDT ionization energies for acetylene in the CBS limit.

TABLE VI. Total ground state energy (hartree) and vertical and adiabatic ionization energies (eV) of benzene.

Method	${}^1\tilde{X}$	${}^2E_{1g}$	${}^2E_{2g}$	${}^2A_{2u}$	${}^2B_{2g}$	${}^2B_{3g}$
CCSD	-231.753 913	9.274	12.384	12.883	9.125	9.594
EOM-CCSD		9.316	12.169	12.663	9.182	9.626
CCSD(<i>f</i> T)	-231.799 191	9.335	12.173	12.599	9.170	9.615
EOM-CCSD(<i>f</i> T)		9.070	11.973	12.308	8.920	9.374
CCSD(<i>d</i> T)	-231.803 784	9.336	12.143	12.543	9.169	9.611
EOM-CCSD(<i>d</i> T)		9.044	11.958	12.279	8.894	9.349
EOM-CC(2,3)		8.982	11.821	11.992		
Expt. ^a		9.45	11.7	12.3		

^aFrom Ref. 77.

sponding (2,3) values by 0.1–0.2 eV. The absolute error for the (2,3) values for the energy differences between the ionized states with respect to the experimental data⁷⁸ ranges from 0.003 to 0.05 eV.

G. Adenine

Table VIII gives the vertical and adiabatic SD and the (*x*T) IEs of adenine computed using the reduced cc-pVTZ basis set. The respective MOs are given in the supplementary materials.⁶⁰ All theoretical IEs are too low relative to the experimental values. The (*f*T) values are lower than the SD ones by 0.2–0.3 eV, and (*d*T) reduces them further by about 0.02 eV. However, the trend for theoretical values is the same as for thymine and other examples. The (*x*T) adiabatic IE is larger than the (2,3) one by ~ 0.1 eV and, as in thymine and other examples, this lies between the SD and (2,3) IEs. The (*x*T) correction increases the energy gaps between the ionized states by 0.01–0.02 eV. The SD maximum error for the energy gaps between the ionized states is 0.212 eV. The corresponding values for (*f*T) and (*d*T) are 0.240 and 0.244 eV, respectively. In view of the uncertainties with the experimental values, it is difficult to make a definite conclusion about the accuracy of theoretical methods.

We also calculated the SD IEs using the cc-pVTZ basis set. Assuming that the reduction in basis set has no signifi-

cant effect on the (*x*T) corrections, we extrapolate the (*x*T) IEs for the cc-pVTZ basis set using the energy-additivity formula:

$$\text{IE}_{(xT)}(\text{cc-pVTZ}) = \text{IE}_{(xT)}(\text{cc-pVTZ}_{\text{red}}) + \text{IE}_{\text{SD}}(\text{cc-pVTZ}) - \text{IE}_{\text{SD}}(\text{cc-pVTZ}_{\text{red}}). \quad (34)$$

For the extrapolated *x*T/cc-pVTZ values, the errors for energy differences between the ionized states do not change significantly. The SD and the extrapolated (*f*T) and (*d*T) errors for the cc-pVTZ basis set are 0.216, 0.239, and 0.246 eV, respectively.

IV. CONCLUSIONS

This work presents formalism and implementation of non-iterative perturbative triples correction to the EOM-IP-CCSD wave functions. We neglect the ground-state correction to avoid the imbalance in the description of the closed-shell and ionized states, which results in underestimation of the IEs, as in the case of EOM-IP-CC(2,3). The (*x*T) values are consistently in between the SD and (2,3) values for all the systems considered in this study. The benchmark calculations of the IEs of nitrogen, carbon monoxide, and acetylene indicate that the (*f*T) correction yields the IEs that are the closest to EOM-IP-CCSDT, as compared to the SD, (*d*T), SD*, and (2,3) methods. The respective error bars are 0.2 and

TABLE VII. Vertical and adiabatic ionization energies (eV) of thymine.

Method	$1\ {}^2A'$	$2\ {}^2A'$	$3\ {}^2A'$	$1\ {}^2A''$	$2\ {}^2A''$	$3\ {}^2A''$	${}^2A''_{\text{adia}}$
cc-pVTZ							
EOM-CCSD	10.134	11.038	13.818	9.131	10.516	12.669	8.902
EOM-CCSD(<i>f</i> T)	9.824	10.715	13.529	8.785	10.185	12.284	8.567
EOM-CCSD(<i>d</i> T)	9.793	10.688	13.517	8.763	10.155	12.177	8.545
Reduced cc-pVTZ ^a							
EOM-CCSD	10.030	10.939	13.755	9.026	10.396	12.563	8.813
EOM-CCSD(<i>f</i> T)	9.743	10.638	13.487	8.706	10.088	12.201	8.505
EOM-CCSD(<i>d</i> T)	9.710	10.607	13.473	8.682	10.055	12.174	8.481
EOM-CC(2,3)	9.521	10.397	13.296	8.594	9.921	11.971	8.400
Expt. ^b	9.95	10.80		9.02	10.40	12.10	8.80
Expt. ^c	10.03	10.82		9.18	10.39	12.27	
Expt. ^d	10.05	10.88		9.20	10.44	12.30	

^aThe cc-pVTZ basis with *f*-functions dropped from C, N, and O and *d*-function dropped from H.^bFrom Refs. 78 and 79.^cFrom Ref. 80.^dFrom Ref. 81.

TABLE VIII. Vertical and adiabatic ionization energies (eV) of adenine.

Method	1 ² A	2 ² A	3 ² A	4 ² A	5 ² A	6 ² A	² A _{adia}
Reduced cc-pVTZ ^a							
EOM-CCSD	8.267	9.304	9.491	10.346	10.458	11.389	8.052
EOM-CCSD(<i>f</i> T)	7.976	9.070	9.208	10.105	10.191	11.126	7.766
EOM-CCSD(<i>d</i> T)	7.960	9.052	9.190	10.091	10.174	11.114	7.747
EOM-CC(2,3)							7.660
cc-pVTZ ^a							
EOM-CCSD	8.370	9.377	9.600	10.420	10.576	11.468	8.122
EOM-CCSD(<i>f</i> T) ^b	8.079	9.143	9.317	10.179	10.309	11.205	7.836
EOM-CCSD(<i>d</i> T) ^b	8.063	9.125	9.299	10.165	10.292	11.193	7.817
Expt. ^c	8.48		9.6		10.5	11.39	8.26

^aThe cc-pVTZ basis with *f*-functions dropped from C, N, and O and *d*-function dropped from H.

^bExtrapolated values.

^cFrom Refs. 80 and 92.

1 eV for the principal and satellite states, respectively. The (*x*T) correction lowers the SD IEs of satellite states by several eV and covers about 75% of the error in SD IEs with respect to the SDT benchmark values. The trend of SD, (*f*T)-(*d*T), (2,3) IEs is also observed in the case of thymine and adenine.

The SD, (*f*T), and (*d*T) errors for the excitation energies of the thymine cation versus the experimental values (which have rather large error bars) are 0.467, 0.415, and 0.419 eV, respectively, whereas for adenine these values are 0.212, 0.240, and 0.244 eV. For adenine and thymine, the accuracy of (*x*T) is very similar, however, calculations with a larger basis set are required for converged values. The IEs of benzene are also lowered by 0.3 eV by the (*x*T) corrections. The (*x*T) reduces the ΔE versus EOM-IP difference from 0.26 to 0.026 eV for the $\pi \rightarrow \pi^*$ (vertical) transition in benzene.

For Koopmans' IEs, the mean absolute errors of SD, (*f*T), (*d*T), and SD* with respect to the SDT values are 0.17, 0.10, 0.11, and 0.17 eV, respectively, and the standard deviations are 0.11 for SD and 0.12 for (*x*T) and SD*. For the energy differences between the ionized states, the standard deviations with respect to SDT are 0.14, 0.11, and 0.10 for SD, (*x*T), and SD*, respectively, whereas the mean absolute error is 0.11 eV for all the methods. The SD, (*f*T), and (*d*T) mean absolute errors for energy gaps in the ionized states of benzene and thymine with respect to CC(2,3) benchmark are 0.090, 0.066, and 0.062 eV, respectively, whereas the standard deviations are 0.130, 0.076, and 0.071 eV.

ACKNOWLEDGMENTS

This work was conducted under the auspices of the iOpenShell Center for Computational Studies of Electronic Structure and Spectroscopy of Open-Shell and Electronically Excited Species (iopenshell.usc.edu) supported by the National Science Foundation through the CRIF:CRF Grant No. CHE-0625419+0624602+0625237. We also gratefully acknowledge support of the National Science Foundation through Grants No. CHE-0616271 (AIK) and CHE-0710146 (JFS). We wish to thank Dr. Ksenia Bravaya for providing the geometries of thymine and adenine.

APPENDIX A: IMPLEMENTATION

As follows from Eq. (24), the calculation of noniterative energy correction involves contraction of three five-index tensors, $\tilde{\sigma}$, σ , and D^m . Explicit calculation of these tensors leads to N^6 disk requirements. Therefore, the efficient implementation should avoid explicit calculation of the five-index quantities and directly compute the respective contributions to the energy. To make an efficient use of our block-tensor library,^{82,83} which was designed to handle large tensors and incorporates spatial and spin symmetry, we break down the tensors into smaller arrays of reduced dimensionality tensors by so-called unrolling. For example, instead of generating a five-index block-tensor of type *ijkab*, one can form an *ijk* array of *ab* block tensors. We use uppercase letters to denote the unrolled indices, e.g., $\sigma_{ab}(IJK)$, $\tilde{\sigma}_{ab}(IJK)$, and $D_{ab}^m(IJK)$ represent the *IJK*-unrolled σ_{ijk}^{ab} , $\tilde{\sigma}_{ijk}^{ab}$, and D_{ijkab}^m tensors from Eq. (24). In this notation, the energy correction assumes the following form:

$$E_m^{(2)} = - \frac{1}{3!2!} \sum_{IJK} \sum_{ab} \frac{\tilde{\sigma}_{ab}(IJK)\sigma_{ab}(IJK)}{D_{ab}^m(IJK)}, \quad (\text{A1})$$

and is calculated as follows: for each *IJK*, the reduced dimensionality block tensors $\sigma_{ab}(IJK)$, $\tilde{\sigma}_{ab}(IJK)$, and $D_{ab}^m(IJK)$ are computed, contracted as specified by Eq. (34), and discarded. This implementation takes full advantage of spatial and spin-symmetry.

The $\tilde{\sigma}$ vectors from Eq. (34) are:

$$\tilde{\sigma}_{ab}(IJK) = \langle \Phi_0 L_1 | \bar{H} | \Phi_{IJK}^{ab} \rangle + \langle \Phi_0 L_2 | \bar{H} | \Phi_{IJK}^{ab} \rangle, \quad (\text{A2})$$

where

$$\langle \Phi_0 L_1 | \bar{H} | \Phi_{IJK}^{ab} \rangle = (l_I \langle JK || ab \rangle - l_J \langle IK || ab \rangle + l_K \langle IJ || ab \rangle), \quad (\text{A3})$$

$$\begin{aligned}
\langle \Phi_0 L_2 | \bar{H} | \Phi_{IJK}^{ab} \rangle &= P(ab) (l_{JK}^b F_{Ia} - l_{IK}^b F_{Ja} + l_{IJ}^b F_{Ka}) \\
&- P(ab) \sum_l (l_{IJ}^a l_{JKl}^b - l_{JK}^a l_{IKl}^b + l_{IK}^a l_{Jl}^b) \\
&+ P(ab) \sum_d (l_{IJ}^d l_{Kdab}^7 - l_{IK}^d l_{Jdab}^7 + l_{JK}^d l_{Idab}^7).
\end{aligned} \tag{A4}$$

Thus, the calculation of the above terms requires the following unrolled integrals and intermediates: l_I , l_{JK}^d , l_{IJ}^a , $\langle JK || ab \rangle$, l_{JKl}^b , and l_{Kdab}^7 , which are obtained from the corresponding intermediates^{5,8,4,85} by unrolling. The equations for $\sigma_{ab}(IJK)$ are easily derived in a similar fashion.

$$\tilde{\sigma}_{ab}(IJK) = \langle \Phi_{IJK}^{ab} | \bar{H} | R_1 \Phi_0 \rangle + \langle \Phi_{IJK}^{ab} | \bar{H} | R_2 \Phi_0 \rangle, \tag{A5}$$

where

$$\begin{aligned}
\langle \Phi_{IJK}^{ab} | \bar{H} | R_1 \Phi_0 \rangle &= \sum_l (t_{II}^{ab} H_{JKl}^2 - t_{JI}^{ab} H_{IKl}^2 + t_{KI}^{ab} H_{Jl}^2) \\
&+ P(ab) \sum_d (t_{IJ}^{ad} H_{Kdab}^3 + t_{JK}^{ad} H_{Idb}^3 - t_{IK}^{ad} H_{Jdb}^3),
\end{aligned} \tag{A6}$$

$$\begin{aligned}
\langle \Phi_{IJK}^{ab} | \bar{H} | R_2 \Phi_0 \rangle &= + P(ab) \sum_l (r_{II}^a l_{JKl}^2 - r_{JI}^a l_{IKl}^2 + r_{KI}^a l_{Jl}^2) \\
&+ \sum_l (t_{II}^{ab} H_{JKl}^4 - t_{JI}^{ab} H_{IKl}^4 + t_{KI}^{ab} H_{Jl}^4) \\
&- \sum_d (r_{IJ}^d l_{Kdab}^3 - r_{IK}^d l_{Jdab}^3 + r_{JK}^d l_{Idab}^3) \\
&- P(ab) \sum_d (t_{IJ}^{ad} H_{Kdab}^5 - t_{IK}^{ad} H_{Jdb}^5 + t_{JK}^{ad} H_{Idb}^5).
\end{aligned} \tag{A7}$$

The diagonal is calculated in a slightly different manner. The diagonal expression can be divided into IJK , ab , and

TABLE IX. R -independent intermediates used in the (dT) and (fT) energy expressions.

$$\begin{aligned}
F_{ia} &= f_{ia} + \sum_{jb} t_{ij}^b |ab\rangle \\
F_{ij} &= f_{ij} + \sum_a t_{ia}^a f_{ja} + \sum_k t_{ka}^a \langle jk || ia \rangle + \sum_{kab} t_{ia}^a t_{kb}^b \langle jk || ab \rangle + \\
&\quad \frac{1}{2} \sum_{kbc} t_{ik}^{bc} \langle jk || bc \rangle \\
F_{ab} &= f_{ab} - \sum_i t_{ia}^a f_{ib} - \sum_i t_{ia}^a \langle ia || bc \rangle + \sum_{ijc} t_{ia}^a t_{ij}^c \langle ij || bc \rangle - \\
&\quad \frac{1}{2} \sum_{jkc} t_{ik}^{ac} \langle jk || bc \rangle \\
I_{iab}^1 &= \langle ia || jb \rangle - \sum_k t_{ka}^b \langle jk || ia \rangle - \sum_c t_{ic}^c \langle jb || ac \rangle + \sum_{kc} t_{ia}^c t_{kb}^c \langle jk || ac \rangle - \\
&\quad \sum_{kc} t_{ik}^{bc} \langle jk || ac \rangle \\
I_{ijka}^2 &= -\langle ij || ka \rangle + 2 \sum_l t_{il}^a t_{ijkl}^a + \\
&+ P(ij) \sum_b (t_{ij}^b \langle jb || ka \rangle - \sum_{lc} t_{jl}^{ac} \langle kl || bc \rangle) \\
&- \sum_{b,c} t_{ij}^b t_{ka}^c \langle ka || bc \rangle - \sum_{lbc} t_{il}^b t_{jk}^{ac} \langle kl || bc \rangle \\
&+ \sum_c t_{ij}^{bc} f_{kc} - \frac{1}{2} \sum_{cd} t_{ij}^{cd} \langle kb || cd \rangle + P(ij) \sum_{lc} t_{il}^{bc} \langle jc || kl \rangle \\
I_{icab}^3 &= -\langle ic || ab \rangle + 2 \sum_d t_{id}^d t_{icad}^d + \\
&+ P(bc) \sum_j (t_{ij}^b \langle ia || jc \rangle - \sum_{ad} t_{ik}^{cd} \langle jk || ad \rangle) - \sum_{jk} t_{ij}^b t_{ka}^c \langle jk || ia \rangle - \sum_{jkd} t_{ik}^{ad} \langle jk || ad \rangle \\
&+ \sum_k t_{ik}^{ab} f_{kc} - \frac{1}{2} \sum_{kl} t_{ik}^{ab} \langle ic || kl \rangle + P(ab) \sum_{kad} t_{ik}^{ad} \langle kb || cd \rangle \\
I_{ijkl}^4 &= \frac{1}{2} \langle ij || kl \rangle - \frac{1}{2} P(ij) \sum_a t_{ia}^a \langle kl || ja \rangle + \frac{1}{2} \sum_{ab} t_{ia}^a t_{bj}^b \langle kl || ab \rangle \\
&+ \frac{1}{4} \sum_{cd} t_{ij}^{cd} \langle kl || cd \rangle \\
I_{abcd}^5 &= \frac{1}{2} \langle ab || cd \rangle - \frac{1}{2} \sum_i (t_{ia}^a \langle ib || cd \rangle - t_{ia}^a \langle ia || cd \rangle) + \frac{1}{2} \sum_{ij} t_{ia}^a t_{ij}^b \langle ij || cd \rangle + \frac{1}{4} \sum_{kl} t_{ik}^{ab} \langle kl || cd \rangle \\
I_{ijka}^6 &= \langle ij || ka \rangle - \sum_c t_{ic}^c \langle j || ac \rangle \\
I_{iabc}^7 &= \langle ia || bc \rangle - \sum_j t_{ij}^a \langle ij || bc \rangle
\end{aligned}$$

TABLE X. H-intermediates used in the (dT) and (fT) energy expressions.

$$\begin{aligned}
H_{jkl}^2 &= 2 \sum_m t_{jklm}^4 r_m \\
H_{kdb}^3 &= \sum_l t_{kdlb}^1 r_l \\
H_{ijl}^4 &= P(ij) \sum_{ma} t_{ma}^6 l_{mia}^{ca} r_{jm}^{ca} \\
H_{kdc}^5 &= 1/2 \sum_{mn} t_{mn}^6 t_{mnd}^{bc} r_{mn}^e + \sum_{le} t_{lced}^7 r_{kl}^e
\end{aligned}$$

$IJKab$ parts. The IJK term is just a number and is computed inside the IJK loop. The ab part is calculated once and is then used whenever required. The part depending on both IJK and ab is generated for every IJK , similar to calculation of $\tilde{\sigma}_{ab}(IJK)$ described above. The diagonal can thus be written as

$$D_{ab}^m(IJK) = (Dijk(IJK) - \omega_m) + Dab^{ab} + \tilde{D}_{ab}(IJK), \tag{A8}$$

where

$$Dijk(IJK) = -F_{II} - F_{JJ} - F_{KK} + 2I_{IIJ}^4 + 2I_{IKIK}^4 + 2I_{JKJK}^4, \tag{A9}$$

$$Dab^{ab} = P(ab) F_{aa} + 2I_{abab}^5,$$

$$\begin{aligned}
\tilde{D}_{ab}(IJK) &= -P(ab) (I_{Iala}^1 + I^1 JaJa + I_{KaKa}^1) \\
&- P(ab) \sum_d (t_{IJ}^{ad} \langle IJ || ad \rangle + t_{IK}^{ad} \langle IK || ad \rangle) \\
&+ t_{JK}^{ad} \langle JK || ad \rangle - \sum_l (t_{II}^{ab} \langle II || ab \rangle + t_{JI}^{ab} \langle JI || ab \rangle) \\
&+ t_{KI}^{ab} \langle KI || ab \rangle).
\end{aligned} \tag{A10}$$

The diagonal is symmetric with respect to index permutation, unlike $\tilde{\sigma}$ and σ , which are antisymmetric.

The SD* correction of Saeh and Stanton⁴¹ can be derived from the (fT) correction by keeping only the terms linear in T_2 in the intermediates used for computing $\tilde{\sigma}$ and σ and dropping all the T_1 -containing terms.

The EOM-IP-CCSD(fT), EOM-IP-CCSD(dT), and EOM-IP-CCSD* energy expressions using the above scheme are implemented within the Q-CHEM electronic structure package.⁷⁰

APPENDIX B: INTERMEDIATES IN THE PROGRAMMABLE EXPRESSIONS

Tables IX and X present the programmable expressions for the intermediates used to in the expressions for $\tilde{\sigma}$, σ , and the denominator in the energy equation, Eq. (24). Some of the intermediates are given in the earlier work of Krylov and co-workers.^{5,58,84,85}

¹ D. J. Rowe, *Rev. Mod. Phys.* **40**, 153 (1968).

² K. Emrich, *Nucl. Phys. A.* **351**, 379 (1981).

³ J. Geertsen, M. Rittby, and R. J. Bartlett, *Chem. Phys. Lett.* **164**, 57 (1989).

⁴ J. F. Stanton and R. J. Bartlett, *J. Chem. Phys.* **98**, 7029 (1993).

⁵ S. V. Levchenko and A. I. Krylov, *J. Chem. Phys.* **120**, 175 (2004).

⁶ J. F. Stanton and J. Gauss, *J. Chem. Phys.* **101**, 8938 (1994).

⁷ M. Nooijen and R. J. Bartlett, *J. Chem. Phys.* **102**, 3629 (1995).

⁸ J. F. Stanton and J. Gauss, *Theor. Chim. Acta* **93**, 303 (1996).

⁹ S. R. Gwaltney, M. Nooijen, and R. J. Bartlett, *Chem. Phys. Lett.* **248**, 189 (1996).

¹⁰ M. Nooijen and R. J. Bartlett, *J. Chem. Phys.* **107**, 6812 (1997).

¹¹ S. R. Gwaltney and R. J. Bartlett, *J. Chem. Phys.* **110**, 62 (1999).

- ¹²M. Nooijen and V. Lotrich, *J. Chem. Phys.* **113**, 494 (2000).
- ¹³S. Hirata, M. Nooijen, I. Grabowski, and R. J. Bartlett, *J. Chem. Phys.* **114**, 3919 (2001).
- ¹⁴M. Wladyslawski and M. Nooijen, *ACS Symp. Ser.* **828**, 65 (2002).
- ¹⁵K. W. Sattelmeyer, H. F. Schaefer, and J. F. Stanton, *Chem. Phys. Lett.* **378**, 42 (2003).
- ¹⁶P. D. Fan, M. Kamyia, and S. Hirata, *J. Chem. Theory Comput.* **3**, 1036 (2007).
- ¹⁷P. A. Pieniazek, S. A. Arnstein, S. E. Bradforth, A. I. Krylov, and C. D. Sherrill, *J. Chem. Phys.* **127**, 164110 (2007).
- ¹⁸H. J. Monkhorst, *Int. J. Quantum Chem., Quantum Chem. Symp.* **11**, 421 (1977).
- ¹⁹D. Mukherjee and P. K. Mukherjee, *Chem. Phys.* **39**, 325 (1979).
- ²⁰H. Sekino and R. J. Bartlett, *Int. J. Quantum Chem., Quantum Chem. Symp.* **26**, 255 (1984).
- ²¹H. Koch, H. J. Aa. Jensen, P. Jørgensen, and T. Helgaker, *J. Chem. Phys.* **93**, 3345 (1990).
- ²²M. Head-Gordon and T. J. Lee, in *Modern Ideas in Coupled Cluster Theory*, edited by R. J. Bartlett (World Scientific, Singapore, 1997).
- ²³H. Nakatsuji and K. Hirao, *J. Chem. Phys.* **68**, 2053 (1978).
- ²⁴H. Nakatsuji, *Chem. Phys. Lett.* **177**, 331 (1991).
- ²⁵M. Haque and D. Mukherjee, *J. Chem. Phys.* **80**, 5058 (1984).
- ²⁶D. Sinha, D. Mukhopadhyay, and D. Mukherjee, *Chem. Phys. Lett.* **129**, 369 (1986).
- ²⁷S. Pal, M. Rittby, R. J. Bartlett, D. Sinha, and D. Mukherjee, *Chem. Phys. Lett.* **137**, 273 (1987).
- ²⁸I. Lindgren and D. Mukherjee, *Phys. Rep.* **151**, 93 (1987).
- ²⁹D. Mukherjee and S. Pal, *Adv. Quantum Chem.* **20**, 291 (1989).
- ³⁰D. Mukhopadhyay, S. Mukhopadhyay, R. Chaudhuri, and D. Mukherjee, *Theor. Chim. Acta* **80**, 441 (1991).
- ³¹H. Larsen, K. Hald, J. Olsen, and P. Jørgensen, *J. Chem. Phys.* **115**, 3015 (2001).
- ³²J. F. Stanton, K. W. Sattelmeyer, J. Gauss, M. Allan, T. Skalicky, and T. Bally, *J. Chem. Phys.* **115**, 1 (2001).
- ³³L. V. Slipchenko and A. I. Krylov, *J. Chem. Phys.* **117**, 4694 (2002).
- ³⁴P. A. Pieniazek, A. I. Krylov, and S. E. Bradforth, *J. Chem. Phys.* **127**, 044317 (2007).
- ³⁵J. F. Stanton, *J. Chem. Phys.* **126**, 134309 (2007).
- ³⁶The models with the truncation of EOM amplitudes that is of the same rank as of CC amplitudes or one rank higher are size intensive for IP/EA (but not for EE).
- ³⁷M. Kamiya and S. Hirata, *J. Chem. Phys.* **125**, 074111 (2006).
- ³⁸M. Musiał, S. A. Kucharski, and R. J. Bartlett, *J. Chem. Phys.* **118**, 1128 (2003).
- ³⁹M. Musiał and R. J. Bartlett, *Chem. Phys. Lett.* **384**, 210 (2004).
- ⁴⁰M. Kállay and J. Gauss, *J. Chem. Phys.* **121**, 9257 (2004).
- ⁴¹J. C. Saeh and J. F. Stanton, *J. Chem. Phys.* **111**, 8275 (1999).
- ⁴²S. Hirata, M. Nooijen, and R. J. Bartlett, *Chem. Phys. Lett.* **326**, 255 (2000).
- ⁴³S. Hirata, M. Nooijen, and R. J. Bartlett, *Chem. Phys. Lett.* **328**, 459 (2000).
- ⁴⁴Y. J. Bomble, J. C. Saeh, J. F. Stanton, P. G. Szalay, M. Kállay, and J. Gauss, *J. Chem. Phys.* **122**, 154107 (2005).
- ⁴⁵P. A. Pieniazek, S. E. Bradforth, and A. I. Krylov, *J. Chem. Phys.* **129**, 074104 (2008).
- ⁴⁶S. Pal, M. Rittby, and R. J. Bartlett, *Chem. Phys. Lett.* **160**, 212 (1989).
- ⁴⁷K. Adhikari, S. Chattopadhyay, R. K. Nath, B. K. De, and D. Sinha, *Chem. Phys. Lett.* **474**, 199 (2009).
- ⁴⁸P. U. Manohar and A. I. Krylov, *J. Chem. Phys.* **129**, 194105 (2008).
- ⁴⁹In EOM-IP, EOM-EA, and EOM-SF the reference has different numbers of electrons and is not interacting with the target states at any level of PT.
- ⁵⁰S. R. Gwaltney, C. D. Sherrill, M. Head-Gordon, and A. I. Krylov, *J. Chem. Phys.* **113**, 3548 (2000).
- ⁵¹S. R. Gwaltney and M. Head-Gordon, *J. Chem. Phys.* **115**, 2014 (2001).
- ⁵²K. Raghavachari, G. W. Trucks, J. A. Pople, and M. Head-Gordon, *Chem. Phys. Lett.* **157**, 479 (1989).
- ⁵³J. D. Watts, J. Gauss, and R. J. Bartlett, *J. Chem. Phys.* **98**, 8718 (1993).
- ⁵⁴T. D. Crawford and J. F. Stanton, *Int. J. Quantum Chem.* **70**, 601 (1998).
- ⁵⁵S. A. Kucharski and R. J. Bartlett, *J. Chem. Phys.* **108**, 5243 (1998).
- ⁵⁶P. Piecuch, M. Włoch, J. R. Gour, and A. Kinal, *Chem. Phys. Lett.* **418**, 463 (2005).
- ⁵⁷P. Piecuch and M. Włoch, *J. Chem. Phys.* **123**, 224105 (2005).
- ⁵⁸L. V. Slipchenko and A. I. Krylov, *J. Chem. Phys.* **123**, 084107 (2005).
- ⁵⁹T. H. Dunning, *J. Chem. Phys.* **90**, 1007 (1989).
- ⁶⁰See EPAPS supplementary material <http://dx.doi.org/10.1063/1.3231133> for the molecular structures, total energies, and molecular orbitals.
- ⁶¹D. Feller, *J. Chem. Phys.* **96**, 6104 (1992).
- ⁶²K. A. Peterson, D. E. Woon, and T. H. Dunning, Jr., *J. Chem. Phys.* **100**, 7410 (1994).
- ⁶³J. M. L. Martin, *Chem. Phys. Lett.* **259**, 669 (1996).
- ⁶⁴T. Helgaker, W. Klopper, H. Koch, and J. Noga, *J. Chem. Phys.* **106**, 9639 (1997).
- ⁶⁵A. Halkier, T. Helgaker, P. Jørgensen, W. Klopper, H. Koch, J. Olsen, and A. K. Wilson, *Chem. Phys. Lett.* **286**, 243 (1998).
- ⁶⁶K. L. Bak, P. Jørgensen, J. Olsen, T. Helgaker, and W. Klopper, *J. Chem. Phys.* **112**, 9229 (2000).
- ⁶⁷J. Gauss and J. F. Stanton, *J. Phys. Chem. A* **104**, 2865 (2000).
- ⁶⁸A. A. Golubeva, P. A. Pieniazek, and A. I. Krylov, *J. Chem. Phys.* **130**, 124113 (2009).
- ⁶⁹W. J. Hehre, R. Ditchfield, and J. A. Pople, *J. Chem. Phys.* **56**, 2257 (1972).
- ⁷⁰Y. Shao, L. F. Molnar, Y. Jung, J. Kussmann, C. Ochsenfeld, S. Brown, A. T. B. Gilbert, L. V. Slipchenko, S. V. Levchenko, D. P. O'Neil, R. A. Distasio, Jr., R. C. Lochan, T. Wang, G. J. O. Beran, N. A. Besley, J. M. Herbert, C. Y. Lin, T. Van Voorhis, S. H. Chien, A. Sodt, R. P. Steele, V. A. Rassolov, P. Maslen, P. P. Korambath, R. D. Adamson, B. Austin, J. Baker, E. F. C. Bird, H. Daschel, R. J. Doerksen, A. Drew, B. D. Dunietz, A. D. Dutoi, T. R. Furlani, S. R. Gwaltney, A. Heyden, S. Hirata, C.-P. Hsu, G. S. Kedziora, R. Z. Khallilulin, P. Klunzinger, A. M. Lee, W. Z. Liang, I. Lotan, N. Nair, B. Peters, E. I. Proynov, P. A. Pieniazek, Y. M. Rhee, J. Ritchie, E. Rosta, C. D. Sherrill, A. C. Simmonett, J. E. Subotnik, H. L. Woodcock III, W. Zhang, A. T. Bell, A. K. Chakraborty, D. M. Chipman, F. J. Keil, A. Warshel, W. J. Herberich, H. F. Schaefer III, J. Kong, A. I. Krylov, P. M. W. Gill, and M. Head-Gordon, *Phys. Chem. Chem. Phys.* **8**, 3172 (2006).
- ⁷¹J. F. Stanton, J. Gauss, M. E. Harding, P. G. Szalay, A. A. Auer, R. J. Bartlett, U. Benedikt, C. Berger, D. E. Bernholdt, Y. J. Buomble, O. Christiansen, M. Heckert, O. Heun, C. Huber, T.-C. Jagau, D. Jonsson, J. Jusélius, K. Klein, W. J. Lauderdale, D. A. Matthews, T. Metzroth, D. P. O'Neill, D. R. Price, E. Prochnow, K. Rudd, F. Schiffmann, S. Stopkowitz, M. E. Varner, J. Vázquez, F. Wang, and J. D. Watts, in *CFour*, Coupled Cluster techniques for Computational Chemistry, a quantum-chemical program package, www.cfour.de.
- ⁷²M. E. Harding, T. Metzroth, J. Gauss, and A. A. Auer, *J. Chem. Theory Comput.* **4**, 64 (2008).
- ⁷³K. R. Asmis, T. R. Taylor, and D. M. Neumark, *J. Chem. Phys.* **111**, 8838 (1999).
- ⁷⁴X. Z. Li and J. Paldus, *J. Chem. Phys.* **126**, 224304 (2007).
- ⁷⁵The two leading R_2 amplitudes are degenerate and equal to 0.52 corresponding to ionization of π_u electrons accompanied by $\sigma_u \rightarrow \pi_g$ excitations. The total R_1^2 and R_2^2 values are 0.0232 and 0.9768, respectively.
- ⁷⁶The leading R_2 amplitude is 0.76 corresponding to ionization of a $5a_1$ electron accompanied by excitation of the remaining $5a_1$ electron to one of the degenerate π -LUMO. The total R_1^2 and R_2^2 values are 0.0029 and 0.9971, respectively.
- ⁷⁷P. Baltzer, L. Karlsson, B. Wannberg, G. Ohrwall, D. M. P. Holland, M. A. MacDonald, M. A. Hayes, and D. von Niessen, *Chem. Phys.* **224**, 95 (1997).
- ⁷⁸G. Lauer, W. Schäfer, and A. Schweig, *Tetrahedron Lett.* **16**, 3939 (1975).
- ⁷⁹S. G. Lias, J. E. Bartmess, J. F. Liebman, J. L. Holmes, R. D. Levin, and W. G. Mallard, *J. Phys. Chem. Ref. Data* **17**, 1 (1988).
- ⁸⁰S. Urano, X. Yang, and P. R. LeBrenton, *J. Mol. Struct.* **214**, 315 (1989).
- ⁸¹D. Dougherty, K. Wittel, J. Meeks, and S. P. McGlynn, *J. Am. Chem. Soc.* **98**, 3815 (1976).
- ⁸²A. I. Krylov, C. D. Sherrill, and M. Head-Gordon, "Efficient C++ tensor library for coupled-cluster calculations," (unpublished).
- ⁸³T. L. Windus and J. A. Pople, *Int. J. Quantum Chem.* **56**, 485 (1995).
- ⁸⁴A. I. Krylov, C. D. Sherrill, and M. Head-Gordon, *J. Chem. Phys.* **113**, 6509 (2000).
- ⁸⁵S. V. Levchenko, T. Wang, and A. I. Krylov, *J. Chem. Phys.* **122**, 224106 (2005).

- ⁸⁶ S. Katsumata, K. Kimura, Y. Achiba, T. Yamazaki, and S. Iwata, *Handbook of HeI Photoelectron Spectra of Fundamental Organic Molecules* (Japan Scientific Societies, Tokyo, 1981).
- ⁸⁷ P. Baltzer, M. Larsson, L. Karlsson, B. Wannberg, and M. Carlsson-Götte, *Phys. Rev. A* **46**, 5545 (1992).
- ⁸⁸ S. Svensson, M. Carlsson-Götte, and L. Karlsson, *Phys. Scr.* **44**, 184 (1991).
- ⁸⁹ A. W. Potts and T. A. Williams, *J. Electron Spectrosc. Relat. Phenom.* **3**, 3 (1974).
- ⁹⁰ C. L. French, C. E. Brion, A. O. Bawagan, P. S. Bagus, and E. R. Davidson, *Chem. Phys.* **121**, 315 (1988).
- ⁹¹ R. C. Morrison and G. Liu, *J. Comput. Chem.* **13**, 1004 (1992).
- ⁹² D. Dougherty, E. S. Younathan, R. Voll, S. Abdunur, and S. P. McGlynn, *J. Electron Spectrosc. Relat. Phenom.* **13**, 379 (1978).